JOC The Journal of Organic Chemistry

Article

pubs.acs.org/joc

Understanding the Effects of Bidentate Directing Groups: A Unified Rationale for sp^2 and sp^3 C−H Bond Activations

Hao Tang,[†,‡] Xu-Ri Huang,*[,‡] Jiannian Yao,[†] and Hui Chen*[,†]

[†]Beijing National Laboratory for Molecular Sciences (BNLMS), CAS Key Laboratory of Photochemistry, Institute of Chemistry, Chinese Academy of Sciences, Beijing, 100190, China

[‡]Institute of Theoretical Chemistry, State Key Laboratory of Theoretical and Computational Chemistry, Jilin University, Changchun, 130023, China

Supporting Information

ABSTRACT: Bidentate directing group (DG) strategy is a promising way to achieve sp^2 and more inert sp^3 C−H bond activations in transition metal (TM) catalysis. In this work, we systematically explored the assisting effects exerted by bidentate DGs in the C−H bond activations. Through DFT calculations and well-defined comparative analysis, we for the first time unified the rationale of the reactivity promoted by bidentate DG in sp^2 and sp^3 C−H activations, which are generally consistent with available experimental discoveries about the C−H activation reactivity up to date. In addition to the general rationale of the reactivity, the assisting effects of several typical bidentate DGs were also quantitatively evaluated and compared to reveal their relative promoting ability for C−H activation reactivity. Finally, the effect of the ligating group charge and the position of the ligating group charge in bidentate DGs were also investigated, based on which new types of DGs were designed and proposed to be potentially effective in C−H activation. The deeper understanding and new insight about the bidentate DG strategy gained in this work would help to enhance its further experimental development in sp^2 and sp^3 C−H bond activations.

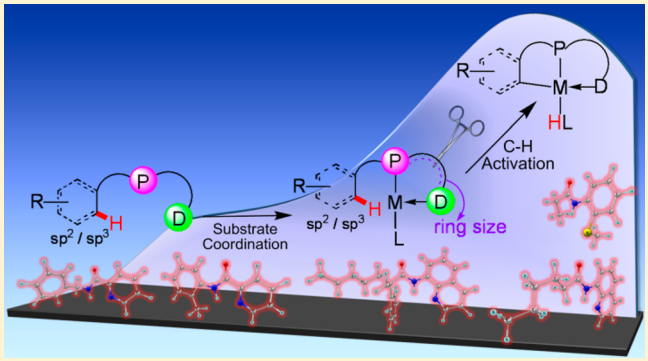

1. INTRODUCTION

Transition-metal-catalyzed selective C−H activation reaction has attracted considerable attention because it provides an unprecedented disconnection strategy for constructing carbon−carbon and carbon−heteroatom bonds.[1] The chelation-assisted transformation is currently recognized as an elegant and versatile approach for the regioselective functionalization of ortho sp^2 and unactivated sp^3 C−H bonds. The directing group (DG) coordinated to the transition metal (TM) can selectively triggers the activation of C−H bond through a cyclometalation reaction.[2] Among the wide varieties of reported DGs, monodentate DGs were utilized in most cases, and their role in C−H activation has been extensively explored both experimentally and computationally.[2−4] In spite of tremendous progress, the development of new types of DGs is still highly desirable to discover new transformations of C−H bonds that cannot be achieved through conventional monodentate DGs. Bidentate-type auxiliary has recently emerged as a new tool in this area because of its versatility and reliability as a DG in many metal-catalyzed C−H bond functionalizations.[5,6] So far, catalytic systems containing *N*,*N*- and *N*,*S*-bidentate DGs, developed by many groups, such as Daugulis, Chen, Yu, Chatani, Miura, Ackermann, Shi, Baran, Nakamura, Ge, and Babu, have been used to activate both C(sp^2)−H bonds[7−12] (Scheme 1A) and more challenging C(sp^3)−H bonds[7c,e−i,13−17] (Scheme 1B).

Similar to the case of C(sp^2)−H bond activation (Scheme 1A), the functionalization of unactivated C(sp^3)−H bonds assisted by bidentate DGs has attracted extensive research interests and efforts (Scheme 1B). In 2005, Daugulis et al. first demonstrated the Pd-catalyzed β-arylation of carboxylic acid and the γ-arylation of amine derivatives by using 8-aminoquinoline (Q) and picolinamide (PA) auxiliaries.[13a] Since this seminal finding, a variety of Pd(II)-catalyzed sp^3 C−H bond activation reactions utilizing *N*,*N*-bidentate DGs have been developed.[13] For example, Chatani et al. has employed Q as bidentate DG for alkynylation of sp^3 C−H bonds.[13h] PA has also been utilized as bidentate DG by Zhang et al. for arylation/oxidation of benzylic C−H bonds.[13v] Many C(sp^3)−H activations promoted by TMs other than Pd have also been shown to benefit from bidentate DGs. Chatani et al. reported on the $Ru_3(CO)_{12}$-catalyzed carbonylation of C(sp^3)−H bonds in aliphatic amides with a pyridinylmethylamino moiety as the bidentate DG.[14] The direct arylation and alkylation of unactivated C(sp^3)−H bonds of aliphatic amides were achieved via nickel catalysis with the assistance of Q as bidentate DG by

Received: March 14, 2015
Published: April 2, 2015

DOI: 10.1021/acs.joc.5b00580
J. Org. Chem. 2015, 80, 4672−4682

Scheme 1. *N,N*- and *N,S*-Bidentate DG Strategy for sp^2 and sp^3 C−H Bond Activations

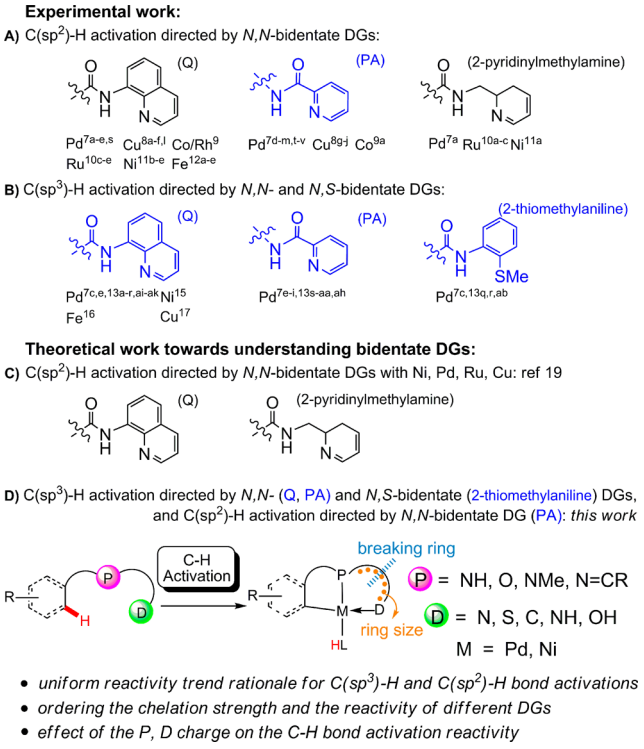

Chatani, Ge, and their co-workers.[15a,b] Nakamura et al. recently reported that Q-based double *N,N*-coordination strategy is crucial for realizing the challenging iron-catalyzed direct arylation of C(sp^3)−H bond.[16] Very recently, the intramolecular dehydrogenative amidation of aliphatic amides, directed by the Q bidentate ligand, was developed by Ge et al. using a copper-catalyzed C(sp^3)−H bond functionalization process.[17a] Moreover, these auxiliaries have been employed by several groups in C(sp^3)−H activation reactions for synthetic purposes. In this regard, Daugulis et al. reported Q-directed synthesis of unnatural amino acids by the efficient β-arylation of C(sp^3)−H of *N*-phthaloylalanine derivatives with iodoarenes.[13b] Corey et al. has used the Q auxiliary to arylate C(sp^3)−H in α-amino acid derivatives.[13g] Notably, the Q- and PA-based bidentate DGs have been recently applied by Chen et al. in arylation of C(sp^3)−H bond to total synthesis of natural product celogentin and (+)-obafluorin, respectively.[13c,s] Carbocycles have also been constructed through the aid of the Q-directed functionalization of C(sp^3)−H bond.[13d]

Despite the remarkable experimental progress in this field, a quantitative understanding of the role played by bidentate DGs in the key step of inert C(sp^3)−H bond activation has not yet been disclosed. Recently, using DFT calculations, we for the first time deciphered the key origins of the C(sp^2)−H bond activation reactivity assisted by *N,N*-bidentate chelation of Q and 2-pyridinylmethylamine DGs, which can explain many previously observed reactivities in experiments involving TMs of Ni, Pd, Ru, and Cu.[19] Our theoretical modeling even predicted the unprecedented reactivity of new substrate, which was confirmed by our combined experimental study.[19] The calculations mainly reveal two key points: (1) Among the two coordinating sites of the *N,N*-bidentate DG, the proximal one influences more the C−H activation barrier $\Delta G^{\ddagger}$, while the distal site affects more the free energy change ΔG relevant to the substrate coordination, and (2) enlarging/shrinking the chelation ring can exert different effects on the reactivity, depending on the metal identity and the ring size. Considering these findings for the reactivity of C(sp^2)−H bond activation, it is intriguing to investigate whether the above effects of the bidentate DGs also exist in C(sp^3)−H bond activation.

Experimentally, various bidentate DGs, in particular those of *N,N*- and *N,S*-bidentate types, have been used as auxiliaries in chelation-assisted transformations of C−H bonds. The attachable and detachable *N,N*-bidentate DGs of 2-pyridinylmethylamine, Q, PA, etc. have been found broadly successful in Pd-,[7,13] Cu,[8,17] Co,[9] Rh,[9] Ru,[10,14] Ni,[11,15] and Fe[12,16] mediated C−H bond activations. Besides the *N,N*-bidentate DGs, the *N,S*- and *N,O*-bidentate auxiliaries have also been employed to direct the C−H bond activations by Pd and Cu.[7c,13q,r,ab,18] Theoretically, however, only two *N,N*-bidentate auxiliaries of 2-pyridinylmethylamine and Q have been explored recently for understanding their role in TM-mediated C(sp^2)−H bonds activation.[19] To the best of our knowledge, there are still no theoretical work for understanding the assistance of PA and *N,S*-bidentate DGs in C−H bonds activation. It is therefore desired to further explore the C−H bond activation reactivity trend with other types of bidentate DGs. Furthermore, it is of note that the bidentate DGs are usually not equally effective for a given sp^2 or sp^3 C−H bond activation reaction in experiment. Thus, deciphering their reactivity differences from theoretical calculations would be helpful for understanding bidentate DGs.

In this paper, based on our original work of C(sp^2)−H bond activation assisted by two *N,N*-bidentate DGs,[19] we explored the roles of three *N,N*-bidentate and one *N,S*-bidentate DGs in typical TM-catalyzed C(sp^3)−H bond activations by performing DFT theoretical calculations. Extending from C(sp^2)−H to C(sp^3)−H bond activation as well as including more types of bidentate DGs successfully enabled us to unify the understanding of the roles played by the bidentate DGs in both sp^2 and sp^3 C−H bond activations for the first time. Moreover, comparison between various bidentate DGs would render the useful information about the chelating and reactivity-promoting abilities of these auxiliaries in C−H bond activations. Additionally, the effect of the charge of the bidentate DGs on the reactivity of the C(sp^2)−H bond activation was also investigated. This comprehensive study can help us to uniformly understand the origin of the reactivity in sp^2 and sp^3 C−H bond activations enabled by the bidentate chelation strategy.

2. METHODS

All DFT calculations were carried out using the Gaussian 09 suite of programs.[20] The geometries of all stationary points on potential energy surfaces (PESs) were fully optimized in gas phase without symmetry constraints by using hybrid B3LYP density functional[21] in combination with def2-SVP basis set[22] (B1) for all the atoms. Harmonic vibrational frequency calculations were performed to verify the nature of the stationary points reported in this work and also to obtain the thermal Gibbs free energy correction. All minima were verified to have no imaginary frequency, whereas all optimized transition states (TSs) were confirmed to have only one proper imaginary frequency. Intrinsic reaction coordinate (IRC) calculations were also conducted to ensure that all the C−H activation TSs connect the corresponding cyclometalated intermediates with the corresponding reactants on PESs. The thermal correction to the Gibbs free energy was calculated at the corresponding experimental reaction temperature of 110, 110, 130, 140, and 50 °C for reactions 1, 2, 3, 4, and 5, respectively. To refine the electronic energy, B3LYP single

DOI: 10.1021/acs.joc.5b00580
J. Org. Chem. 2015, 80, 4672−4682

point calculations with larger def2-TZVP basis set[22] (B2) were carried out on the optimized structures. In all the B2 single point calculations, the continuum solvation model SMD[23] was utilized to take the solvent effect into consideration. The experimentally employed solvents (toluene for reactions 1 and 2, xylene for reaction 3, 2-methyl-2-propanol for reaction 4, and tetrahydrofuran for reaction 5) were used in the solvent effect modeling as the respective solvents. The reported energies in this work include the B2 electronic energy in solution, DFT-D3 empirical dispersion correction (with zero short-range damping scheme) proposed by Grimme et al.,[24] the gas-phase thermal correction to the Gibbs free energy, and solvation free energy correction.

3. RESULTS AND DISCUSSION

In line with the current consensus on the reaction schemes of C−H activation assisted by DGs,[2,3] our basic model for C−H activation is shown in Scheme 2. Quite similar to the

Scheme 2. Reaction Model for sp^2 and sp^3 C−H Activation Utilizing Bidentate Chelation Strategy

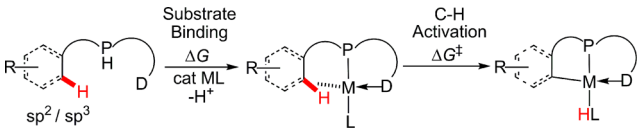

Michaelis−Menten model of classic enzymatic catalysis,[25] in Scheme 2 the substrate first chelates the metal center to form a C−H preactivated intermediate, followed by the C−H bond cleavage. The tendency of this intermediate formation for substrate binding can be measured by the Gibbs coordination free energy change, ΔG, while the kinetic easiness of the cleavage of the C−H bond is characterized by the C−H activation free energy barrier, $\Delta G^{\ddagger}$. As shown in this work, we are able to decipher the origin of the reactivity, compare its chelating ability, and predict viable substrate in C−H bond activation enabled by the bidentate chelation strategy by computing and comparing the two key parameters (ΔG and $\Delta G^{\ddagger}$) of the above reaction model. More detailed discussion of this comparative analysis can be found in our previous work, hence will not be repeated here.[19]

On the basis of the excellent and extensive experimental reports utilizing bidentate chelation strategy,[7c,d,13v,h,15a] we selected the TM-catalyzed C−H bond activations assisted by most representative *N,N*-bidentate (Q, PA), and *N,S*-bidentate (2-thiomethylaniline) DGs. These reactions, as depicted in Scheme 3, include Q-assisted Pd(II)-catalyzed C(sp^3)−H bond activation reaction (1),[13h] PA-assisted Pd(II)-catalyzed C-(sp^3)−H bond activation reaction (2),[13v] *N,S*-assisted Pd(II)-catalyzed C(sp^3)−H bond activation reaction (3),[7c] and Q-assisted Ni(II)-catalyzed C(sp^3)−H bond activation (4).[15a] Moreover, as a typical example of PA-assisted Pd(II)-catalyzed C(sp^2)−H bond activation, reaction (5),[7d] which was not covered in our previous study on C(sp^2)−H bond activations assisted by other *N,N*-bidentate DGs,[19] is also under study to assist the comparison between C(sp^3)−H and C(sp^2)−H activation. In these reactions, the d^8 Pd(II) and Ni(II) complexes adopt the typical four-coordinate square-planar geometry. As shown in Scheme 3, all these reactions (1−5) start with the substrate binding to the metal. Following this preactivation, C−H activation step occurs through a concerted metallacyclization/deprotonation process, with the experimentally employed ligand CH_3COO^- and $MesCOO^-$ acting as the base to accept the proton in Pd- and Ni-catalyzed C−H bond

Scheme 3. Pd- and Ni-Catalyzed C(sp^3)−H and C(sp^2)−H Bond Activations Studied in This Work

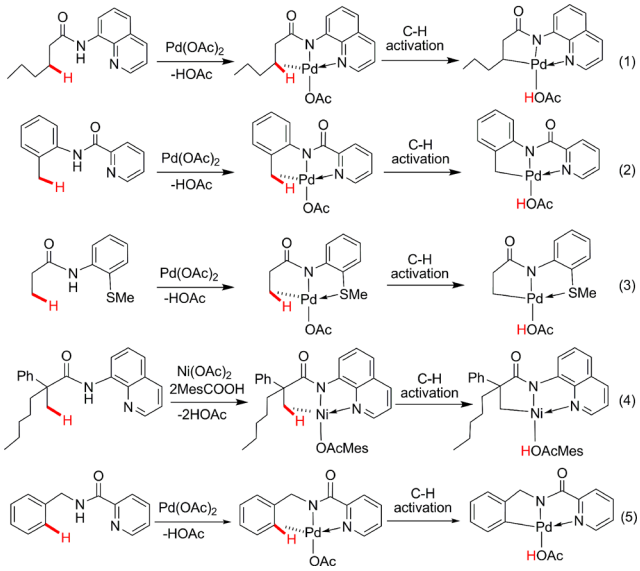

activations, respectively. Concerning the selection of the TMs in above systems, since we had studied Ni, Pd, Cu, and Ru in our previous work on C(sp^2)−H bond activation,[19] here in this work we focus on the more representative Pd and Ni in C(sp^3)−H bond activation. We did not choose Fe mainly because of its obscure reaction mechanism and very complicated open-shell electronic structures likely involved in corresponding C−H bond activation, which is in sharp contrast to the closed-shell electronic structures of above Pd and Ni systems, and deserves detailed investigation for reaction mechanism elsewhere.

According to the structural features of bidentate DG as shown in Scheme 2, i.e., a deprotonative amido ligand at the P (proximal) coordinating site, a strong N/S ligand at the D (distal) coordinating site, and a five-membered metallacycle formed by the bidentate P,D-chelation, here we modeled a series of substrates as displayed in Scheme 4. These substrates are obtained by means of substituting the NH ligand at the P site or the N/S ligand at the D site, enlarging chelation-ring size, and breaking bidentate chelation, with an objective of unraveling the origin of the effectiveness of the bidentate DGs on the reactivity in C(sp^3)−H/C(sp^2)−H bond activations (1−5). Many of these substrates can be taken as solid examples for testing the validity of our theory on C−H activation reactivity, since they have been explored in previous experimental work.[7c,d,13v,h,15a]

In our study for each reaction we choose a substrate that is known to be reactive in experiment as reference. By comparing a specific substrate to the corresponding reference substrate with the aid of the $\Delta\Delta G$ and $\Delta\Delta G^{\ddagger}$ from their ΔG and $\Delta G^{\ddagger}$, we could estimate the relative C−H activation reactivity of different substrates. The reasons for describing the reactivity in a relative manner ($\Delta\Delta G$ and $\Delta\Delta G^{\ddagger}$ from their ΔG and $\Delta G^{\ddagger}$) are that, on the one hand, all the "noises" irrelevant to the substrate binding are canceled in subtraction of two ΔG's to get $\Delta\Delta G$ within one specific reaction system. Given the fact that the difference in the ΔG values to be compared lies only in substrates, $\Delta\Delta G$ obtained thereby can faithfully exhibit the binding energy difference between the different substrates. In this comparative way, confined information on relative

DOI: 10.1021/acs.joc.5b00580
J. Org. Chem. 2015, 80, 4672−4682

Scheme 4. Substrates for Reactions 1−5 Explored in This Work

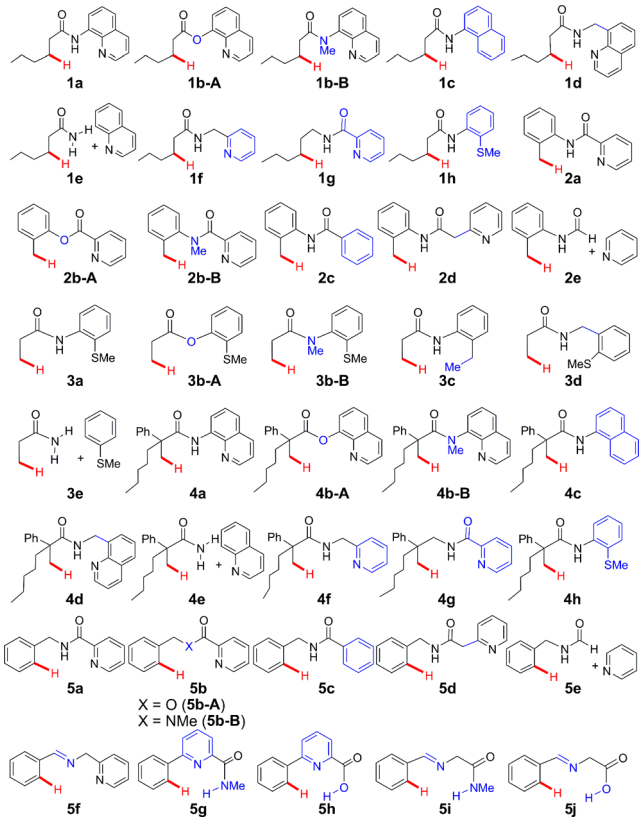

energetics for substrate binding and C−H activation are revealed by $\Delta\Delta G$ and $\Delta\Delta G^{\ddagger}$, respectively. On the other hand, the accuracy limit of current approximate density functionals can be tolerated more in computing the $\Delta\Delta G$ and $\Delta\Delta G^{\ddagger}$ values in this relative manner, since the trends of energetics are more reliably followed in DFT calculations than the values of energetics.[26] Tables 1, 3, and 4 display all the computed results of $\Delta\Delta G$ and $\Delta\Delta G^{\ddagger}$ with the known experimental reactivity denoted to facilitate comparisons between the theory and experiments for Pd- and Ni-catalyzed reactions, and the ΔG and $\Delta G^{\ddagger}$ data are relegated to the SI (see Schemes S1, S2). Below we present several aspects of our results separately, which show that our theoretical understanding is consistent with all the respective previous experimental findings.[7c,d,13v,h,15a]

3.1. The Effectiveness of *N,N*- and *N,S*-Bidentate DGs on the Reactivity of C(sp^3)−H and C(sp^2)−H Bond Activations. *3.1.1. The Effect of Proximal Coordinating Site.* Experimentally, the necessity of the presence of deprotonative amide group at the proximal coordinating site in the C−H activation has been frequently investigated by changing NH in amide group to O or NMe,[7d,r,t,8f,j,l,10a,c,d,f,11b,c,13a,h,o,15a,d,16,18b] which could inhibit the coordination at this site. It was found experimentally that these substitutions in DG part never worked to render any C−H activation reactivity. In order to reveal the origin for the key role of NH in the P position, we examined the O- and NMe-substituted substrates **1b** (**1b-A** and **1b-B**), **2b** (**2b-A** and **2b-B**), **3b** (**3b-A** and **3b-B**), and **4b** (**4b-A** and **4b-B**) in the C(sp^3)−H bond activation processes and **5b** (**5b-A** and **5b-B**) in the C(sp^2)−H bond activation process, as shown in the second and third columns of data in Table 1. Correspondingly, the respective pristine substrates **1a**, **2a**, **3a**, **4a**, and **5a** serve as our references for comparison.

First, concerning NH-to-O substitution, the C(sp^3)−H activation barriers $\Delta G^{\ddagger}$ for O-substituted substrates **1b-A**, **2b-A**, **3b-A**, and **4b-A** in reactions 1−4 are all significantly higher than the corresponding pristine substrates **1a**, **2a**, **3a**, and **4a** by 24.5, 26.0, 25.2, and 26.9 kcal/mol, respectively. In contrast, the Gibbs coordination free energy, ΔG, is much less affected by this O-substitution ($\Delta\Delta G$ = 0.0/1.4/−4.6/−3.6 kcal/mol for **1b-A**/**2b-A**/**3b-A**/**4b-A**). Substrates **3b-A** and **4b-A** even bind catalyst more tightly than the corresponding pristine substrates. This result implies that it is the increase of C−H activation barrier that causes the ineffectiveness of NH-to-O substitution in DG for C(sp^3)−H bond activations. Inspecting the C(sp^2)−H bond activation in reaction 5, **5b-A** exhibits similar reactivity trend as in C(sp^3)−H bond activations, by bearing a substantial increase in activation barriers $\Delta G^{\ddagger}$ ($\Delta\Delta G^{\ddagger}$ = 16.0 kcal/mol) but a small change in substrate binding energy ($\Delta\Delta G$ = 2.1 kcal/mol). These results, combined with the same trend previously found in the C(sp^2)−H bond activations assisted by other *N,N*-bidentate DGs,[19] demonstrates that the C−H activation barrier is the dominant factor causing the unreactive NH-to-O replacement at the P position in both C(sp^3)−H and C(sp^2)−H bond activations. Generally, this consistent trend explains well why experimentally such substitutions in bidentate DGs always led to their ineffectiveness in the C−H bond activation reactions.[7r,8f,j,l,10c,11b,c,15a,d]

Now we turn to NH-to-NMe substitution at the P position of the bidentate DG. Experimentally, when *N*-methyl amide was introduced, the bidentate DGs were never found reactive in corresponding C(sp^3)−H and C(sp^2)−H activation reactions,[7d,r,t,8f,j,l,10a,c,d,f,11b,c,13a,h,o,16,18b] which is consistent with our following computational results. As shown in Table 1, for **1b-B**, **2b-B**, **3b-B**, and **4b-B** with *N*-methyl group at P position, significant increases of the C(sp^3)−H bond activation barriers are observed ($\Delta\Delta G^{\ddagger}$ = 21.9/28.8/34.3/24.7 kcal/mol for **1b-B**/**2b-B**/**3b-B**/**4b-B**), while their substrate bindings are much less affected ($\Delta\Delta G$ = 4.2/−3.2/1.6/−1.7 kcal/mol for **1b-B**/**2b-B**/**3b-B**/**4b-B**). For C(sp^2)−H bond activation, **5b-B** exhibits similar behavior by having substantial increase of activation barrier ($\Delta\Delta G^{\ddagger}$ = 16.9 kcal/mol) and small binding energy change ($\Delta\Delta G$ = −1.3 kcal/mol). This uniform trend found here, as well as the similar trend in the previous C(sp^2)−H bond activation with other *N,N*-bidentate DGs,[19] generally indicates that NH-to-NMe substitution causes malfunction of the bidentate DG predominantly by increasing the C−H activation barrier height rather than weakening the substrate binding.

Combining the above results for NH-to-O and NH-to-NMe substitution in various bidentate DGs for C(sp^3)−H and C(sp^2)−H bond activations, we can generally conclude that P position affects much more the C−H activation barrier rather than the substrate binding. At first sight, this conclusion is somewhat counterintuitive, since NH-to-O and NH-to-NMe substitutions can block the coordination of P site of bidentate DG and intuitively should lead to the loss of the coordinating strength of the substrate. However, this result can find its origin from the structural feature of reactant complex (RC). For example, as depicted in Figure 1, although C−H activation TSs of reaction 1 with substrates **1a**, **1b-A**, and **1b-B** (**TS$_{1a}$**, **TS$_{1b\text{-}A}$**, and **TS$_{1b\text{-}B}$**) are qualitatively similar in structure near the C−H activating moiety, significant differences in geometry exist

DOI: 10.1021/acs.joc.5b00580
J. Org. Chem. 2015, 80, 4672−4682

Table 1. Calculated Relative Substrate Coordination Free Energy Change ($\Delta\Delta G$) and Relative C−H Activation Free Energy Barrier ($\Delta\Delta G^{\ddagger}$) in kcal/mol for C(sp^3)−H/C(sp^2)−H Bond Activation Reactions 1−5[a]

substrate / reaction/DG		1a	1b-A	1b-B	1c	1d	1e
1/Q	$\Delta\Delta G$	0.0[b,g]	0.0[b]	4.2[b,h]	27.1[b,h]	8.4[b]	14.7[b]
Pd sp^3	$\Delta\Delta G^{\ddagger}$	0.0[b,g]	24.5[b]	21.9[b,h]	-1.1[b,h]	-1.9[b]	1.2[b]
substrate / reaction/DG		2a	2b-A	2b-B	2c	2d	2e
2/PA	$\Delta\Delta G$	0.0[c,i]	1.4[c]	-3.2[c]	10.3[c,j]	5.3[c]	14.6[c]
Pd sp^3	$\Delta\Delta G^{\ddagger}$	0.0[c,i]	26.0[c]	28.8[c]	10.0[c,j]	-1.7[c]	1.0[c]
substrate / reaction/DG		3a	3b-A	3b-B	3c	3d	3e
3/N,S	$\Delta\Delta G$	0.0[d,k]	-4.6[d]	1.6[d]	26.8[d]	3.6[d]	13.7[d]
Pd sp^3	$\Delta\Delta G^{\ddagger}$	0.0[d,k]	25.2[d]	34.3[d]	-2.2[d]	0.9[d]	1.7[d]
substrate / reaction/DG		4a	4b-A	4b-B	4c	4d	4e
4/Q	$\Delta\Delta G$	0.0[e,l]	-3.6[e,m]	-1.7[e]	31.3[e,m]	11.0[e]	14.9[e]
Ni sp^3	$\Delta\Delta G^{\ddagger}$	0.0[e,l]	26.9[e,m]	24.7[e]	-1.3[e,m]	0.6[e]	1.9[e]
substrate / reaction/DG		5a	5b-A	5b-B	5c	5d	5e
5/PA	$\Delta\Delta G$	0.0[f,n]	2.1[f]	-1.3[f,o]	21.1[f]	3.8[f]	13.1[f]
Pd sp^2	$\Delta\Delta G^{\ddagger}$	0.0[f,n]	16.0[f]	16.9[f,o]	-1.8[f]	-3.5[f]	-1.0[f]

[a]Compared with the reference reaction, positive $\Delta\Delta G$ and $\Delta\Delta G^{\ddagger}$ mean less favorable binding energy and higher barrier, respectively, and vice versa. [b]ΔG and $\Delta G^{\ddagger}$ of **1a** as reference. [c]ΔG and $\Delta G^{\ddagger}$ of **2a** as reference. [d]ΔG and $\Delta G^{\ddagger}$ of **3a** as reference. [e]ΔG and $\Delta G^{\ddagger}$ of **4a** as reference. [f]ΔG and $\Delta G^{\ddagger}$ of **5a** as reference. [g]Reactive, see ref 13h. [h]Not reactive, see ref 13h. [i]Reactive, see ref 13v. [j]Not reactive, see ref 13v. [k]Reactive, see ref 7c. [l]Reactive, see ref 15a. [m]Not reactive, see ref 15a. [n]Reactive, see ref 7d. [o]Not reactive, see ref 7d.

between their respective RCs (**RC$_{1a}$**, **RC$_{1b\text{-}A}$**, and **RC$_{1b\text{-}B}$**). Due to the anchoring role of the proximal coordinating site, C−H bond to be cleaved in **RC$_{1a}$** adopts a C−H preactivated agostic geometry, while the corresponding C−H bonds in **RC$_{1b\text{-}A}$** and **RC$_{1b\text{-}B}$** without anchoring of the proximal coordinating site are not preactivated and lie far away from the metal center. The absence of C−H preactivation in RC could lead to the increase of C−H activation barrier. To fulfill the stable Pd(II) four-coordinate pattern and to neutralize the charge of RCs, one more anionic acetate ligand is required in **RC$_{1b\text{-}A}$** and **RC$_{1b\text{-}B}$** than in **RC$_{1a}$**, which compensates the binding energy loss caused by the absence of proximal coordination in substrate. This explains why free energy change ΔG associated with substrate binding appears to be quite similar in **RC$_{1a}$**, **RC$_{1b\text{-}A}$**, and **RC$_{1b\text{-}B}$**. This explanation for the effect of proximal site also appears to be the case in reactions 2−5 with different DGs and/or metal for C(sp^3)−H and C(sp^2)−H bond activation (for details see Figures S2c-S 2f, S3c-S 3f, S4c-S 4f, S5c-S 5f in the SI). Irrespective of explanation, all the related computational results in this work invariably suggest that the crucial role of the NH group in terms of the reactivity of the bidentate DGs, as proposed in recent experimental and theoretical investigations.[5,6,7c,d,t,8f,j,10c,f,11b,c,13a,15d,19]

3.1.2. The Effect of Distal Coordinating Site. Next, we sought to evaluate the effect on the distal coordinating site D by changing the DGs without strong coordinating ability. We studied the substrates **1c**, **2c**, **3c**, **4c**, and **5c** in reactions 1−5 wherein the heterocyclic sp^2 nitrogen coordinating atom or thioetheric sp^3 sulfur coordinating atom was replaced by almost noncoordinative sp^2 and sp^3 carbon atoms, respectively. For these substitutions, a trend different from the proximal coordinating site P is discovered. As shown in the fourth column of the data in Table 1, for all reactions except reaction 2, relative to the corresponding pristine substrates **1a**/**3a**/**4a**/

DOI: 10.1021/acs.joc.5b00580
J. Org. Chem. 2015, 80, 4672−4682

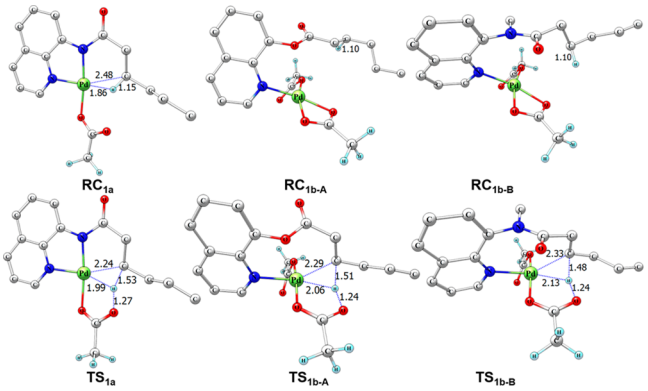

Figure 1. Optimized geometries of reactants and TSs for proximally substituted (by O and NMe) substrates (**RC$_{1b-A}$**, **RC$_{1b-B}$**, **TS$_{1b-A}$**, **TS$_{1b-B}$**) and the pristine substrate **1a** (**RC$_{1a}$**, **TS$_{1a}$**) involved in reaction 1. Hydrogen atoms on the substrates are omitted for clarity, except the transferred H. Unlike the pristine substrate **RC$_{1a}$**, two acetate ligands remain in the proximally substituted systems to make them neutral.

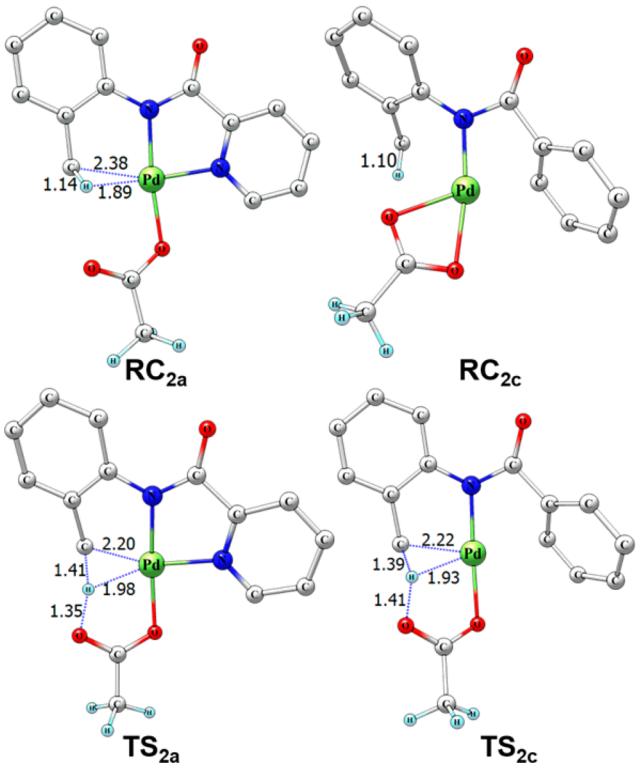

Figure 2. Optimized geometries of reactants and TSs for distally substituted substrate (**RC$_{2c}$**, **TS$_{2c}$**) and the pristine substrate (**RC$_{2a}$**, **TS$_{2a}$**) involved in reaction 2. Hydrogen atoms on the substrates are omitted for clarity except the transferred H atom.

5a, the C−H activation barriers $\Delta G^{\ddagger}$ only change slightly by no more than about 2 kcal/mol ($\Delta\Delta G^{\ddagger}$ = −1.1/−2.2/−1.3/−1.8 kcal/mol for **1c**/**3c**/**4c**/**5c**), while free energy changes ΔG associated with substrate binding increase significantly ($\Delta\Delta G$ = 27.1/26.8/31.3/21.1 kcal/mol for **1c**/**3c**/**4c**/**5c**). This result indicates that the distal site D affects more the substrate binding free energy than the C−H activation barrier. This is in agreement with the available experimental results of the incapability of these substrates in bidentate DG-assisted Pd- and Ni-catalyzed C(sp^3)−H bond activation reactions.[13h,15a] In contrast to P site variations, the D site coordination weakening in bidentate DG-assisted C(sp^3)−H and C(sp^2)−H activation reactions will not necessarily lead to significant increase of C−H activation barriers as evidenced by the fact that all barriers in these reactions arising from the D site replacement are even lowered to some extent. This is in line with the previous theoretical studies on the C(sp^2)−H bond activation reaction.[19]

However, concerning PA-assisted C(sp^3)−H bond activation (reaction 2) with substrate **2c**, different behavior was observed. As shown in Table 1, ΔG and $\Delta G^{\ddagger}$ significantly increase respectively by 10.3 and 10.0 kcal/mol, both of which contributed substantially to the missing reactivity of this reaction with substrate **2c**.[13v] Similar to the case of P site substitution discussed above, this substantial increase in $\Delta G^{\ddagger}$ can be explained by the geometric structure difference between **RC$_{2a}$** and **RC$_{2c}$**. As shown in Figure 2, when the D pyridinyl group is replaced by corresponding phenyl group, TS structure is similar near the C−H activating moiety, while **RC$_{2a}$** and **RC$_{2c}$** adopt quite different geometries. In **RC$_{2a}$**, C−H preactivated agostic structure is obtained, while in **RC$_{2c}$** C−H to be activated is far away from metal center, thus no preactivation occurs. Closely resembling the case of proximal substitution, the absence of C−H preactivation in RC here could also lead to the increase of C−H activation barrier. Combing all results of reactions 1−5, all the related computational results in this work invariably suggest that weakening D coordination site would bring detrimental effect on the reactivity of the bidentate DGs, as found by all relevant experimental investigations up to date.[7t,v,8f,j,l,10a−d,f,11b,c,13h,o,v,w,14b,15a,d,16,18b]

3.1.3. The Effect of Enlarging Chelation Ring. In each pristine substrates (**1a**−**5a**), the chelation of DG is achieved via a five-membered chelation ring involving coordination of P and D sites to metal. It is an interesting issue to explore the effect of the chelation ring size on the cleavage of C(sp^3)−H bond. Hence, the substrates **1d**, **2d**, **3d**, and **4d**, which have one-carbon larger ring compared to the corresponding pristine substrates **1a**, **2a**, **3a**, and **4a**, have been investigated.[27] By inspecting the fifth column of data in Table 1, for these six-membered chelation rings, Pd/Ni-catalyzed C(sp^3)−H bond activation reactions 1−4 utilizing three kinds of bidentate DGs have their substrate binding strength weakened by 8.4, 5.3, 3.6, and 11.0 kcal/mol ($\Delta\Delta G$ = 8.4/5.3/3.6/11.0 kcal/mol for **1d**/**2d**/**3d**/**4d**), respectively. While the corresponding barriers only change by −1.9, −1.7, 0.9, and 0.6 kcal/mol compared with those of the corresponding pristine substrates ($\Delta\Delta G^{\ddagger}$ = −1.9/−1.7/0.9/0.6 kcal/mol for **1d**/**2d**/**3d**/**4d**). These results indicate that it is the Gibbs coordination free energy loss that mainly reduces the efficiency of these C(sp^3)−H activations with the six-membered chelation rings. Concerning Pd-catalyzed C(sp^2)−H activation reaction 5 assisted by PA DG, certain decrease of ΔG by 3.8 kcal/mol was observed, however this decrease is compensated largely by the 3.5 kcal/mol decrease of $\Delta G^{\ddagger}$, which demonstrates that the reactivity is expected to be largely conserved in this case. Similar compensation behavior was also seen in previous theoretical study of a Pd-catalyzed C(sp^2)−H activation assisted by another *N*,*N*-bidentate DG (2-pyridinylmethylamine), whose C−H activation reactivity had been experimentally confirmed by us.[19] Generally, the limited theoretical results in six-membered chelation rings for both C(sp^3)−H and C(sp^2)−H activations show a similar pattern of reactivity regulation by consistently weakening substrate binding strength, while both increasing and decreasing changes exist for C−H activation

DOI: 10.1021/acs.joc.5b00580
J. Org. Chem. 2015, 80, 4672−4682

barrier. This dichotomous picture from our calculations is in line with the previous split experimental results, which indicated that six-membered chelation rings are either reactive[11a,19] or unreactive.[10a−c,14a,b]

3.1.4. The Effect of Chelation. To probe the effect of chelation effect itself in the bidentate DGs, we studied **1e**, **2e**, **3e**, **4e**, and **5e** with no chelation from DGs at all. Consistently, for all C−H bond activation reactions 1−5, as shown in the last column of data in Table 1, it is apparent that the main effect exerted by chelation is to enhance the substrate binding strength of substrates by about 13−15 kcal/mol ($\Delta\Delta G$ = 14.7/14.6/13.7/14.9/13.1 kcal/mol for **1e**/**2e**/**3e**/**4e**/**5e**). The barriers are only slightly affected, without a uniform direction of changes ($\Delta\Delta G^{\ddagger}$ = 1.2/1.0/1.7/1.9/−1.0 kcal/mol for **1e**/**2e**/**3e**/**4e**/**5e**). Generally, this trend here from C(sp^3)−H and C(sp^2)−H activations is same as the previous trend from sp^2-only C−H activations.[19]

To reveal the origin of the significant increase in the substrate binding free energy when bidentate chelation is absent, we analyzed the free energy contributions as shown in Table 2. The computed Gibbs coordination free energy, $\Delta\Delta G$, consists of two components. One is electronic energy component $\Delta\Delta E$, that includes the solvent effect and DFT-D3 dispersion correction, and the other is the thermal Gibbs free energy correction $\Delta\Delta G_{Gibbs}$, that involves the entropic contribution. Results in Table 2 indicate that $\Delta\Delta G_{Gibbs}$ contribution dominates $\Delta\Delta G$ in all reactions 1−5 under study, and the contribution from $\Delta\Delta E$ is very small. This result is again in line with our previous results of C(sp^2)−H activations.[19] Thus, substrate binding benefits from bidentate chelation by free energy factors, most likely to be the entropic one.

Table 2. Calculated Components ($\Delta\Delta G_{Gibbs}$ and $\Delta\Delta E$) of Relative Free Energy ($\Delta\Delta G$) for Substrates 1e, 2e, 3e, 4e, and 5e (in kcal/mol) without the Bidentate Chelation[a]

	substrate/DG				
	1e/Q[b]	**2e**/PA[c]	**3e**/N,S[d]	**4e**/Q[e]	**5e**/PA[f]
$\Delta\Delta G_{Gibbs}$	14.2	15.6	14.8	15.8	15.3
$\Delta\Delta E$	0.5	−1.0	−1.1	−0.9	−2.2
$\Delta\Delta G$	14.7	14.6	13.7	14.9	13.1

[a]$\Delta\Delta G = \Delta\Delta G_{Gibbs} + \Delta\Delta E$, wherein $\Delta\Delta G_{Gibbs}$ is the gas-phase thermal free energy correction component of Gibbs free energy, and $\Delta\Delta E$ is the electronic energy (in solution, including DFT-D3 dispersion correction) component of Gibbs free energy. [b]Taking **1a** as reference in reaction 1. [c]Taking **2a** as reference in reaction 2. [d]Taking **3a** as reference in reaction 3. [e]Taking **4a** as reference in reaction 4. [f]Taking **5a** as reference in reaction 5.

3.2. Comparison of Bidentate DGs. In our previous work on C(sp^2)−H activation, we compared two *N*,*N*-bidentate DGs (Q and 2-pyridinylmethylamine) and found that substrates with Q consistently have tighter binding with metal than the corresponding substrates with 2-pyridinylmethylamine.[19] Here in this work with one more *N*,*N*-bidentate DG (PA) and one *N*,*S*-bidentate DG (2-thiomethylaniline), it would be interesting to compare these four representative bidentate DGs altogether. In particular, the chelation abilities (ΔG), the C−H cleavage barriers ($\Delta G^{\ddagger}$), and the effective barrier (sum of ΔG and $\Delta G^{\ddagger}$) related to the relative C−H activation reactivity can be determined.

Experimentally, in the Q-assisted Pd-catalyzed C(sp^3)−H bond activation (reaction 1), **1a** with Q is reactive, but **1f**, **1g**, and **1h** with the other bidentate auxiliaries were found to be unreactive.[13f] The computational results in Table 3 show that the Gibbs coordination free energies ΔG for **1f**, **1g**, and **1h** are 2.1, 2.3, and 4.7 kcal/mol higher than the pristine substrates **1a**, and the C−H activation barriers $\Delta G^{\ddagger}$ change by 1.3, 1.0, −2.1 kcal/mol, respectively. In total, the effective barrier increases by 3.4, 3.3, and 2.6 kcal/mol for **1f**, **1g**, and **1h**, indicating that PA, 2-thiomethylaniline, and 2-pyridinylmethylamine are all inferior to Q in this Pd-catalyzed C(sp^3)−H bond activation. Hence our results are in full agreement with the reactivity trend found in experiment.[13f]

Table 3. Calculated $\Delta\Delta G$ and $\Delta\Delta G^{\ddagger}$ (in kcal/mol) for C(sp^3)−H Bond Activation Reactions 1 and 4, with Four Bidentate DGs (Q, PA, 2-thiomethylaniline, and 2-pyridinylmethylamine)[a]

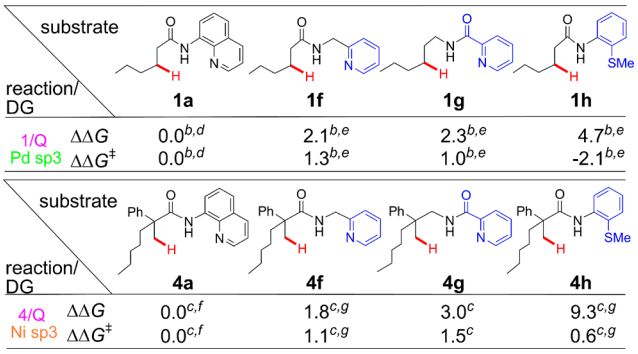

[a]Compared with the reference reaction, positive $\Delta\Delta G$ and $\Delta\Delta G^{\ddagger}$ mean less favorable binding energy and higher barrier, respectively, and vice versa. [b]ΔG and $\Delta G^{\ddagger}$ of **1a** as reference. [c]ΔG and $\Delta G^{\ddagger}$ of **4a** as reference. [d]Reactive, see ref 13h. [e]Not reactive, see ref 13h. [f]Reactive, see ref 15a. [g]Not reactive, see ref 15a.

For Ni-catalyzed C(sp^3)−H bond activation with the assistance of Q (reaction 4), as shown in Table 3, both ΔG and $\Delta G^{\ddagger}$ for **4f**, **4g**, and **4h** are found to be higher than the pristine substrate **4a**, especially for the one with 2-thiomethylaniline (**4h**). In total, the calculated effective barrier increases relative to **4a** for substrates **4f**, **4g**, and **4h** are 2.9, 4.5, and 9.9 kcal/mol, respectively. Considering this energetic result, we conclude that Q should be superior to the other three alternative DGs. Again, the superiority of Q (**4a**) over other bidentate auxiliaries such as in **4f**, **4g**, and **4h**, is consistent with the experimental results that Q could successfully assist Ni-catalyzed C(sp^3)−H bond activation reaction, but 2-pyridinylmethylamine and 2-thiomethylaniline could not.[15a] Combining above results for Pd and Ni, we conclude that Q binds to metal more tightly than the other three representative alternatives in C(sp^3)−H bond activations. This tighter binding of Q and the reactivity superiority generated thereby are in line with our previous study for C(sp^2)−H activations.[19] Here we note that the magnitude of binding difference could sometimes become quite metal-dependent as shown in *N*,*S*-bidentate DG for Ni and Pd.

3.3. The Effect of the Negative Charge and Charge Position of Bidentate DG on the Reactivity in PA-assisted C(sp^2)−H Bond Activation. In all the four representative bidentate DGs discussed above, the P position has a deprotonative amide group and hence bears negative

DOI: 10.1021/acs.joc.5b00580
J. Org. Chem. 2015, 80, 4672−4682

charge when binding with metal, while the D position has a neutral ligating group. This feature stimulates us to explore the effect associated with the charge of bidentate DG on the C−H activation reactivity. As a result we designed several new substrates for reaction 5 based on **5a** as shown in Table 4,

Table 4. Calculated ΔΔ*G* and ΔΔ*G*‡ (in kcal/mol) for PA-assisted C(sp²)−H Bond Activation Reaction 5, with Bidentate DGs Designed to Reveal the Effect of the Negative Charge and Charge Position of Bidentate DG[a]

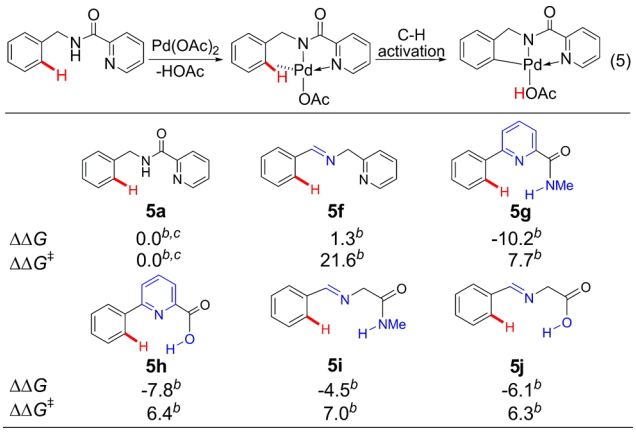

[a]Compared with the reference reaction, positive ΔΔ*G* and ΔΔ*G*‡ mean less favorable binding energy and higher barrier, respectively, and vice versa. [b]Δ*G* and Δ*G*‡ of **5a** as reference. [c]Reactive, see ref 7d.

including one P-D neutral−neutral substrate (**5f**) and four P-D neutral-negative substrates (**5g**, **5h**, **5i**, **5j**). The calculated relative Δ*G* and Δ*G*‡ (labeled ΔΔ*G* and ΔΔ*G*‡) for the corresponding substrates are displayed in Table 4, taking **5a** as reference.

3.3.1. The Effect of the Ligand Charge at the Proximal Coordinating Site. As shown in Table 4, deprotonative amide ligating group at the P site in **5a** was replaced by a neutral imine ligating group in **5f**. The calculated large increase of C−H activation barrier Δ*G*‡ by more than 20 kcal/mol implies that **5f** is not likely to be reactive in the reaction, in spite of the almost unaffected substrate binding (ΔΔ*G* = 1.3 kcal/mol for **5f**) strength.

Similar to the cases of proximally substituted substrates in the C(sp³)−H and C(sp²)−H bond activations, the large activation barrier increase of **5f** relative to **5a** can find its origin from its character of RC geometry in reaction 5. In contrast to $\mathbf{RC_{5a}}$, as depicted in Figure 3, $\mathbf{RC_{5f}}$ disfavors the C−H preactivated Pd-CH agostic geometry. Due to the neutral character of ligating groups at both P and D sites in **5f**, the second anionic acetate coordination is more energetically favored than for **5a**. As a result, imine at P site cannot ligate Pd in $\mathbf{RC_{5f}}$, which makes the imine group fail to act as an anchoring group for the C−H bond to be cleaved. Inspection of TSs in Figure 3 indicates that $\mathbf{TS_{5f}}$ and $\mathbf{TS_{5a}}$ is qualitatively similar in structure near the C−H activating moiety, which implies that TS is unlikely to cause the large barrier difference between **5f** and **5a**.

3.3.2. The Effect of the Ligand Charge at the Distal Coordinating Site. Having shown the detrimental effect of charge neutralization at P site on the C−H activation, we now turn to the D site. Here we are particularly interested in exploring the effect of changing the deprotonative ligating group from P site to D site. To clarify this issue, as shown in

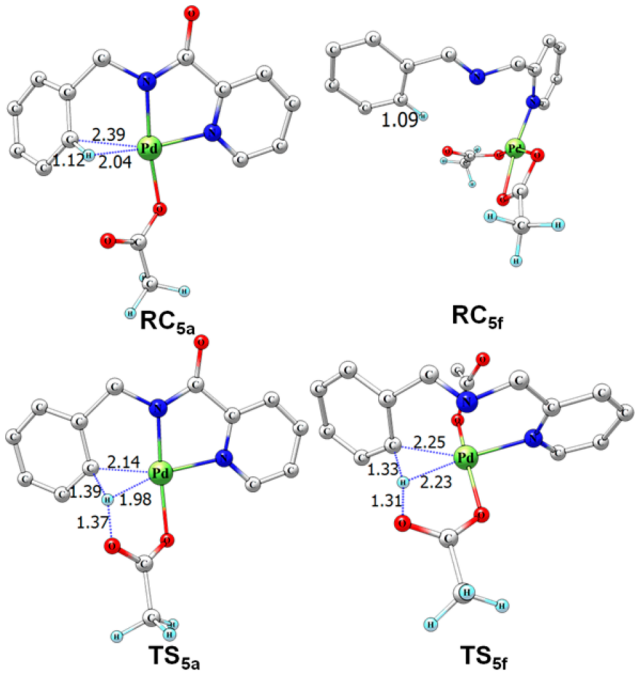

Figure 3. Optimized geometries of RCs and TSs for substrate **5f** ($\mathbf{RC_{5f}}$, $\mathbf{TS_{5f}}$) and the pristine substrate **5a** ($\mathbf{RC_{5a}}$, $\mathbf{TS_{5a}}$) involved in reaction 5. Hydrogen atoms on the substrates are omitted for clarity, except the transferred H. Unlike the pristine substrate $\mathbf{RC_{5a}}$, two acetate ligands remain in the reaction for **5f** to make the system neutral.

Table 4, we studied four substrates **5g**, **5h**, **5i**, and **5j**, all with a negatively charged ligating group at the D site.

First, compared with **5a**, the P-D positions of pyridine and amide ligating groups are exchanged in **5g**. Further changing the amide ligating group to a carboxylate one produces **5h**. For **5g** and **5h**, the substrate binding Gibbs free energies are favored by 10.2 and 7.8 kcal/mol than **5a**, respectively, while the C−H activation barriers are increased by 7.7 and 6.4 kcal/mol, as shown in Table 4. In total, effective C−H activation barriers are lowered by 2.5 and 1.4 kcal/mol, which shows that **5g** and **5h** could be reactive substrates in this C(sp²)−H activation (reaction 5). Changing pyridine ligating group in **5g** and **5h** to imine group will generate **5i** and **5j**, respectively. For these two substrates, substrate binding free energy is disfavored by a few kcal/mol compared with **5g** and **5h**, indicating that coordination strength of imine is weaker than that of pyridine. However, the C−H activation barriers of **5i** and **5j** are almost unaffected in comparison with **5g** and **5h**. Overall, these results for **5g**, **5h**, **5i**, and **5j** indicate that moving the negatively charged ligating group from P site to D site often can favor the substrate binding but increase the C−H activation barrier, the sum effect of which may still afford reactive substrates in C−H activation.

4. CONCLUSIONS

In this work, we theoretically analyzed the effects exerted by several typical bidentate DGs on C−H bond activations. Three representative *N*,*N*-bidentate DGs (Q, PA, 2-pyridinylmethylamine) and one *N*,*S*-bidentate DG (2-thiomethylaniline) are systematically explored in Pd- and Ni-catalyzed C(sp³)−H and C(sp²)−H bond activations by DFT calculations. Using an informative theoretical approach based on comparative analysis of the substrate Gibbs coordination free energy and the C−H

DOI: 10.1021/acs.joc.5b00580
J. Org. Chem. 2015, 80, 4672−4682

activation barrier, we for the first time are able to reach a uniform understanding of the assisting role played by bidentate DGs in activations of both C(sp^2)−H and more inert C(sp^3)−H bonds. The unified rationale concerning the bidentate DGs for the C−H activation reactivity includes: (1) The proximal coordinating site of the bidentate DGs generally influences the C−H activation barrier more, while the distal coordinating site affects more the Gibbs coordination free energy; (2) enlarging the chelation ring of bidentate DGs from a five- to six-membered one causes significant loss of substrate binding free energy; and (3) bidentate chelation in bidentate DGs generally leads to a tighter substrate binding. In addition to the above general rationale for many bidentate DGs, the comparison between different bidentate DGs reveals that Q (8-aminoquinoline) auxiliary could provide more superior assistance for sp^2 and sp^3 C−H bonds activation than the other bidentate DGs, mainly because it generally makes the substrate bind the central metals more tightly.

To reveal the effects of the charge of the bidentate DGs, we have designed several new bidentate DGs based on PA-assisted C(sp^2)−H bond activation. When two ligating groups are changed from the normal P-D negative-neutral one to both-neutral one in bidentate DG, our calculation indicates significant increase of the C−H activation barrier, which makes the bidentate DG ineffective. However, when the charges of the P-D coordinating sites are exchanged from the negative-neutral one to the neutral-negative one, the resultant bidentate DGs are often found to favor the substrate binding though increasing the C−H activation barrier, the sum effect of which may still make bidentate DGs effective in C−H activation. This constitutes a promising idea to design new bidentate DGs in future.

Our results and rationale for C−H activation reactivity are generally in agreement with all the relevant experimental results. The general rationale behind bidentate DG-assisted TM-catalyzed sp^2 and sp^3 C−H bond activations in this work may be helpful to the deeper understanding of the bidentate DG strategy, which is the basis for designing new and more effective bidentate DGs used for sp^2 and sp^3 C−H bonds activations.

■ ASSOCIATED CONTENT

Supporting Information

Detailed calculated energies, all optimized geometries, and Cartesian coordinates. This material is available free of charge via the Internet at http://pubs.acs.org.

■ AUTHOR INFORMATION

Corresponding Authors

*E-mail: chenh@iccas.ac.cn.

*E-mail: huangxr@jlu.edu.cn.

Notes

The authors declare no competing financial interest.

■ ACKNOWLEDGMENTS

Generous financial supports from the National Natural Science Foundation of China (21290194, 21221002, 21473215) and Institute of Chemistry, CAS, are gratefully acknowledged.

■ REFERENCES

(1) For some recent reviews of C−H bond functionalization, see: (a) Lersch, M.; Tilset, M. *Chem. Rev.* **2005**, *105*, 2471−2526. (b) Kakiuchi, F.; Kochi, T. *Synthesis* **2008**, 3013−3039. (c) McGlacken, G. P.; Bateman, L. M. *Chem. Soc. Rev.* **2009**, *38*, 2447−2464. (d) Daugulis, O.; Do, H.-Q.; Shabashov, D. *Acc. Chem. Res.* **2009**, *42*, 1074−1086. (e) Chen, X.; Engle, K. M.; Wang, D.-H.; Yu, J.-Q. *Angew. Chem., Int. Ed.* **2009**, *48*, 5094−5115. (f) Ackermann, L.; Vicente, R.; Kapdi, A. R. *Angew. Chem., Int. Ed.* **2009**, *48*, 9792−9826. (g) Colby, D. A.; Bergman, R. G.; Ellman, J. A. *Chem. Rev.* **2010**, *110*, 624−655. (h) Sehnal, P.; Taylor, R. J. K.; Fairlamb, I. J. S. *Chem. Rev.* **2010**, *110*, 824−889. (i) Wendlandt, A. E.; Suess, A. M.; Stahl, S. S. *Angew. Chem., Int. Ed.* **2011**, *50*, 11062−11087. (j) Ackermann, L. *Chem. Commun.* **2010**, *46*, 4866−4877. (k) Mkhalid, I. A. I.; Barnard, J. H.; Marder, T. B.; Murphy, J. M.; Hartwig, J. F. *Chem. Rev.* **2010**, *110*, 890−931. (l) Sun, C.-L.; Li, B.-J.; Shi, Z.-J. *Chem. Rev.* **2011**, *111*, 1293−1314. (m) Chen, D. Y.-K.; Youn, S. W. *Chem.-Eur. J.* **2012**, *18*, 9452−9474. (n) Yamaguchi, J.; Yamaguchi, A. D.; Itami, K. *Angew. Chem., Int. Ed.* **2012**, *51*, 8960−9009. (o) Li, B.-J.; Shi, Z.-J. *Chem. Soc. Rev.* **2012**, *41*, 5588−5598. (p) Newhouse, T.; Baran, P. S. *Angew. Chem., Int. Ed.* **2011**, *51*, 3362−3374. (q) Kuhl, N.; Hopkinson, M. N.; Wencel-Delord, J.; Glorius, F. *Angew. Chem., Int. Ed.* **2012**, *51*, 10236−10254. (r) Boorman, T. C.; Larrosa, I. *Chem. Soc. Rev.* **2011**, *40*, 1910−1925. (s) Collet, F.; Lescot, C.; Dauban, P. *Chem. Soc. Rev.* **2011**, *40*, 1926−1936. (t) Cho, S. H.; Kim, J. Y.; Kwak, J.; Chang, S. *Chem. Soc. Rev.* **2011**, *40*, 5068−5083. (u) Che, C.-M.; Lo, V. K.-Y.; Zhou, C.-Y.; Huang, J.-S. *Chem. Soc. Rev.* **2011**, *40*, 1950−1975. (v) Mousseau, J.; Charette, A. B. *Acc. Chem. Res.* **2013**, *46*, 412−424. (w) Kozhushkov, S. I.; Ackermann, L. *Chem. Sci.* **2013**, *4*, 886−896.

(2) (a) Murai, S.; Kakiuchi, F.; Sekine, S.; Tanaka, Y.; Kamatani, A.; Sonoda, M.; Chatani, N. *Nature* **1993**, *366*, 529−531. (b) Ritleng, V.; Sirlin, C.; Pfeffer, M. *Chem. Rev.* **2002**, *102*, 1731−1769. (c) Daugulis, O.; Zaitsev, V. G.; Shabashov, D.; Pham, Q. N.; Lazareva, A. *Synlett* **2006**, 3382−3388. (d) Alberico, D.; Scott, M. E.; Lautens, M. *Chem. Rev.* **2007**, *107*, 174−238. (e) Lyons, T. W.; Sanford, M. S. *Chem. Rev.* **2010**, *110*, 1147−1169. (f) Ackermann, L. *Chem. Rev.* **2011**, *111*, 1315−1345. (g) Yeung, C. S.; Dong, V. M. *Chem. Rev.* **2011**, *111*, 1215−1292. (h) Neufeldt, S. R.; Sanford, M. S. *Acc. Chem. Res.* **2012**, *45*, 936−946. (i) Engle, K. M.; Mei, T. S.; Wasa, M.; Yu, J.-Q. *Acc. Chem. Res.* **2012**, *45*, 788−802. (j) Colby, D. A.; Tsai, A. S.; Bergman, R. G.; Ellman, J. *Acc. Chem. Res.* **2012**, *45*, 814−825. (k) Arockiam, P. B.; Bruneau, C.; Dixneuf, P. H. *Chem. Rev.* **2012**, *112*, 5879−5918. (l) Wang, C. *Synlett* **2013**, *24*, 1606−1613.

(3) For a recent general review on computational studies, see: Balcells, D.; Clot, E.; Eisenstein, O. *Chem. Rev.* **2010**, *110*, 749−823 and references therein.

(4) Some selected theoretical studies on monodentate DGs: (a) Matsubara, T.; Koga, N.; Musaev, D. G.; Morokuma, K. *J. Am. Chem. Soc.* **1998**, *120*, 12692−12693. (b) Davies, D. L.; Donald, S. M. A.; Macgregor, S. A. *J. Am. Chem. Soc.* **2005**, *127*, 13754−13755. (c) Zhou, B.; Chen, H.; Wang, C. *J. Am. Chem. Soc.* **2013**, *135*, 1264−1267. (d) Clot, E.; Chen, J.; Lee, D.-H.; Sung, S. Y.; Appelhans, L. N.; Faller, J. W.; Crabtree, R. H.; Eisenstein, O. *J. Am. Chem. Soc.* **2004**, *126*, 8795−8804.

(5) Rouquet, G.; Chatani, N. *Angew. Chem., Int. Ed.* **2013**, *52*, 11726−11743.

(6) Corbet, M.; De Campo, F. *Angew. Chem., Int. Ed.* **2013**, *52*, 9896−9898.

(7) C(sp^2)−H activation, Pd: (a) Ano, Y.; Tobisu, M.; Chatani, N. *Org. Lett.* **2012**, *14*, 354−357. (b) Kanyiva, K. S.; Kuninobu, Y.; Kanai, M. *Org. Lett.* **2014**, *16*, 1968−1971. (c) Shabashov, D.; Daugulis, O. *J. Am. Chem. Soc.* **2010**, *132*, 3965−3972. (d) Gou, F.-R.; Wang, X.-C.; Huo, P.-F.; Bi, H.-P.; Guan, Z.-H.; Liang, Y.-M. *Org. Lett.* **2009**, *11*, 5726−5729. (e) Nadres, E. T.; Santos, G. I. F.; Shabashov, D.; Daugulis, O. *J. Org. Chem.* **2013**, *78*, 9689−9714. (f) Nadres, E. T.; Daugulis, O. *J. Am. Chem. Soc.* **2012**, *134*, 7−10. (g) He, G.; Zhao, Y.; Zhang, S.; Lu, C.; Chen, G. *J. Am. Chem. Soc.* **2012**, *134*, 3−6. (h) Zhang, S.-Y.; He, G.; Zhao, Y.; Wright, K.; Nack, W. A.; Chen, G. *J. Am. Chem. Soc.* **2012**, *134*, 7313−7316. (i) Nack, W. A.; He, G.; Zhang, S.-Y.; Lu, C. X.; Chen, G. *Org. Lett.* **2013**, *15*, 3440−3443. (j) Zhao, Y.; Chen, G. *Org. Lett.* **2011**, *13*, 4850−4853. (k) He, G.; Lu, C.; Zhao, Y.; Nack, W. A.; Chen, G. *Org. Lett.* **2012**, *14*, 2944−2947.

DOI: 10.1021/acs.joc.5b00580
J. Org. Chem. 2015, 80, 4672−4682

(l) Zhao, Y.; He, G.; Nack, W. A.; Chen, G. *Org. Lett.* **2012**, *14*, 2948−2951. (m) Liu, C.; Zhang, S.-Y.; He, G.; Nack, W. A.; Chen, G. *Tetrahedron* **2014**, *70*, 4197−4203. (n) Mei, T.-S.; Leow, D.; Xiao, H.; Laforteza, B. N.; Yu, J.-Q. *Org. Lett.* **2013**, *15*, 3058−3061. (o) Shang, M.; Sun, S.-Z.; Dai, H.-X.; Yu, J.-Q. *J. Am. Chem. Soc.* **2014**, *136*, 3354−3357. (p) Chen, F.-J.; Zhao, S.; Hu, F.; Chen, K.; Zhang, Q.; Zhang, S.-Q.; Shi, B.-F. *Chem. Sci.* **2013**, *4*, 4187−4192. (q) Ye, X. H.; He, Z. R.; Ahmed, T.; Weise, K.; Akhmedov, N. G.; Petersen, J. L.; Shi, X. D. *Chem. Sci.* **2013**, *4*, 3712−3716. (r) Ye, X. H.; Shi, X. D. *Org. Lett.* **2014**, *16*, 4448−4451. (s) Deb, A.; Bag, S.; Kancherla, R.; Maiti, D. *J. Am. Chem. Soc.* **2014**, *136*, 13602−13605. (t) Iwasaki, M.; Kaneshika, W.; Tsuchiya, Y.; Nakajima, K.; Nishihara, Y. *J. Org. Chem.* **2014**, *79*, 11330−11338. (u) Huang, L.; Li, Q.; Wang, C.; Qi, C. *J. Org. Chem.* **2013**, *78*, 3030−3038. (v) Huang, L.; Sun, X. D.; Li, Q.; Qi, C. *J. Org. Chem.* **2014**, *79*, 6720−6725. (w) Cross, W. B.; Hope, E. G.; Lin, Y.-H.; Macgregor, S. A.; Singh, K.; Solan, G. A.; Yahya, N. *Chem. Commun.* **2013**, *49*, 1918−1920.

(8) C(sp^2)−H activation, Cu: (a) Tran, L. D.; Popov, I.; Daugulis, O. *J. Am. Chem. Soc.* **2012**, *134*, 18237−18240. (b) Tran, L. D.; Roane, J.; Daugulis, O. *Angew. Chem., Int. Ed.* **2013**, *52*, 6043−6046. (c) Truong, T.; Klimovica, K.; Daugulis, O. *J. Am. Chem. Soc.* **2013**, *135*, 9342−9345. (d) Daugulis, O.; Roane, J. *Org. Lett.* **2013**, *15*, 5842−5845. (e) Suess, A. M.; Ertem, M. Z.; Gramer, C. J.; Stahl, S. S. *J. Am. Chem. Soc.* **2013**, *135*, 9797−9804. (f) Nishino, M.; Hirano, K.; Satoh, T.; Miura, M. *Angew. Chem., Int. Ed.* **2013**, *52*, 4457−4461. (g) Odani, R.; Hirano, K.; Satoh, T.; Miura, M. *J. Org. Chem.* **2013**, *78*, 11045−11052. (h) Takamatsu, K.; Hirano, K.; Satoh, T.; Miura, M. *Org. Lett.* **2014**, *16*, 2892−2895. (i) Li, X.; Liu, Y.-H.; Gu, W.-J.; Li, B.; Chen, F.-J.; Shi, B.-F. *Org. Lett.* **2014**, *16*, 3904−3907. (j) Li, Q.; Zhang, S.-Y.; He, G.; Ai, Z.; Nack, W. A.; Chen, G. *Org. Lett.* **2014**, *16*, 1764−1767. (k) Shang, M.; Sun, S.-Z.; Wang, H.-L.; Laforteza, B. N.; Dai, H.-X.; Yu, J.-Q. *Angew. Chem., Int. Ed.* **2014**, *53*, 10439−10442. (l) Wang, S.; Guo, R.; Wang, G.; Chen, S.-Y.; Yu, X.-Q. *Chem. Commun.* **2014**, *50*, 12718−12721. (m) Liu, J.; Zhuang, S.; Gui, Q.; Chen, X.; Yang, Z.; Tan, Z. *Adv. Synth. Catal.* **2015**, *357*, 732−738. (n) Liu, J.; Yu, L.; Zhuang, S.; Gui, Q.; Chen, X.; Wang, W.; Tan, Z. *Chem. Commun.* **2015**, *51*, 6418−6421.

(9) C(sp^2)−H activation, Co, Rh: (a) Daugulis, O.; Grigorjeva, L. *Angew. Chem., Int. Ed.* **2014**, *53*, 10209−10212. (b) Daugulis, O.; Grigorjeva, L. *Org. Lett.* **2014**, *16*, 4688−4690. (c) Daugulis, O.; Grigorjeva, L. *Org. Lett.* **2014**, *16*, 4684−4687. (d) Shibata, K.; Chatani, N. *Org. Lett.* **2014**, *16*, 5148−5151. C(sp^3)−H activation, by Co, see: (e) Wu, X.; Yang, K.; Zhao, Y.; Sun, H.; Li, G.; Ge, H. *Nat. Commun.* **2015**, *6*, 6462.

(10) C(sp^2)−H activation, Ru: (a) Inoue, S.; Shiota, H.; Fukumoto, Y.; Chatani, N. *J. Am. Chem. Soc.* **2009**, *131*, 6898−6899. (b) Shibata, K.; Hasegawa, N.; Fukumoto, Y.; Chatani, N. *ChemCatChem* **2012**, *4*, 1733−1736. (c) Aihara, Y.; Chatani, N. *Chem. Sci.* **2013**, *4*, 664−670. (d) Rouquet, G.; Chatani, N. *Chem. Sci.* **2013**, *4*, 2201−2208. (e) Allu, S.; Swamy, K. C. K. *J. Org. Chem.* **2014**, *79*, 3963−3972. (f) Mamari, H. H. A.; Diers, E.; Ackermann, L. *Chem.-Eur. J.* **2014**, *20*, 9739−9743.

(11) C(sp^2)−H activation, Ni: (a) Shiota, H.; Ano, Y.; Ahihara, Y.; Fukumoto, Y.; Chatani, N. *J. Am. Chem. Soc.* **2011**, *133*, 14952−14955. (b) Ahihara, Y.; Chatani, N. *J. Am. Chem. Soc.* **2013**, *135*, 5308−5311. (c) Yokota, A.; Aihara, Y.; Chatani, N. *J. Org. Chem.* **2014**, *79*, 11922−11932. (d) Cong, X.; Li, Y.; Zeng, X. *Org. Lett.* **2014**, *16*, 3926−3929. (e) Aihara, Y.; Tobisu, M.; Fukumoto, Y.; Chatani, N. *J. Am. Chem. Soc.* **2014**, *136*, 15509−15512. (f) Yang, K.; Wang, Y.; Chen, X.; Kadi, A. A.; Fun, H.-K.; Sun, H.; Zhang, Y.; Lu, H. *Chem. Commun.* **2015**, *51*, 3582−3585. (g) Yan, S.-Y.; Liu, Y.-J.; Liu, B.; Liu, Y.-H.; Shi, B.-F. *Chem. Commun.* **2015**, *51*, 4069−4072. (h) Lin, C.; Li, D.; Wang, B.; Yao, J.; Zhang, Y. *Org. Lett.* **2015**, *17*, 1328−1331.

(12) C(sp^2)−H activation, Fe: (a) Asako, S.; Ilies, L.; Nakamura, E. *J. Am. Chem. Soc.* **2013**, *135*, 17755−17757. (b) Matsubara, T.; Asako, S.; Ilies, L.; Nakamura, E. *J. Am. Chem. Soc.* **2014**, *136*, 646−649. (c) Ilies, L.; Matsubara, T.; Ichikawa, S.; Asako, S.; Nakamura, E. *J. Am. Chem. Soc.* **2014**, *136*, 13126−13129. (d) Fruchey, E. R.; Monks, B. M.; Cook, S. P. *J. Am. Chem. Soc.* **2014**, *136*, 13130−13133. (e) Monks, B. M.; Fruchey, E. R.; Cook, S. P. *Angew. Chem., Int. Ed. Engl.* **2014**, *53*, 11065−11069. (f) Gu, Q.; Al Mamari, H. H.; Graczyk, K.; Diers, E.; Ackermann, L. *Angew. Chem., Int. Ed.* **2014**, *53*, 3868−3871.

(13) C(sp^3)−H activation, Pd: (a) Zaitsev, V.; Shabashov, D.; Daugulis, O. *J. Am. Chem. Soc.* **2005**, *127*, 13154−13155. (b) Tran, L. D.; Daugulis, O. *Angew. Chem., Int. Ed.* **2012**, *51*, 5188−5191. (c) Feng, Y.; Chen, G. *Angew. Chem., Int. Ed.* **2010**, *49*, 958−961. (d) Feng, Y.; Wang, Y.; Landgraf, B.; Liu, S.; Chen, G. *Org. Lett.* **2010**, *12*, 3414−3417. (e) Zhang, S.-Y.; Li, Q.; He, G.; Nack, W. A.; Chen, G. *J. Am. Chem. Soc.* **2013**, *135*, 12135−12141. (f) He, G.; Zhang, S.-Y.; Nack, W. A.; Li, Q.; Chen, G. *Angew. Chem., Int. Ed.* **2013**, *52*, 11124−11128. (g) Reddy, B. V. S.; Reddy, L. R.; Corey, E. J. *Org. Lett.* **2006**, *8*, 3391−3394. (h) Ano, Y.; Tobisu, M.; Chatani, N. *J. Am. Chem. Soc.* **2011**, *133*, 12984−12986. (i) Gutekunst, W. R.; Gianatassio, R.; Baran, P. S. *Angew. Chem., Int. Ed.* **2012**, *51*, 7507−7510. (j) Gutekunst, W. R.; Baran, P. S. *J. Org. Chem.* **2014**, *79*, 2430−2452. (k) Chen, K.; Hu, F.; Zhang, S.-Q.; Shi, B.-F. *Chem. Sci.* **2013**, *10*, 3906−3911. (l) Parella, R.; Gopalakrishnan, B.; Babu, S. A. *J. Org. Chem.* **2013**, *78*, 11911−11934. (m) Pan, F.; Shen, P.-X.; Zhang, L.-S.; Wang, X.; Shi, Z.-J. *Org. Lett.* **2013**, *15*, 4758−4761. (n) Shan, G.; Yang, X.; Zong, Y.; Rao, Y. *Angew. Chem., Int. Ed.* **2013**, *52*, 13606−13610. (o) Wei, Y.; Tang, H.; Cong, X.; Rao, B.; Wu, C.; Zeng, X. *Org. Lett.* **2014**, *16*, 2248−2251. (p) Hoshiya, N.; Kobayashi, T.; Arisawa, M.; Shuto, S. *Org. Lett.* **2013**, *15*, 6202−6205. (q) Parella, R.; Gopalakrishnan, B.; Babu, S. A. *Org. Lett.* **2013**, *15*, 3238−3241. (r) Ting, C. P.; Maimone, T. J. *Angew. Chem., Int. Ed.* **2014**, *53*, 3115−3119. (s) He, G.; Chen, G. *Angew. Chem., Int. Ed.* **2011**, *50*, 5192−5196. (t) Zhang, S.-Y.; He, G.; Nack, W. A.; Zhao, Y.; Li, Q.; Chen, G. *J. Am. Chem. Soc.* **2013**, *135*, 2124−2127. (u) Li, Q.; Zhang, S.-Y.; He, G.; Nack, W. A.; Chen, G. *Adv. Synth. Catal.* **2014**, *356*, 1544−1548. (v) Xie, Y.; Yang, Y.; Huang, L.; Zhang, X.; Zhang, Y. *Org. Lett.* **2012**, *14*, 1238−1241. (w) Ju, L.; Yao, J.; Wu, Z.; Liu, Z.; Zhang, Y. *J. Org. Chem.* **2013**, *78*, 10821−10831. (x) Roman, D. S.; Charette, A. B. *Org. Lett.* **2013**, *15*, 4394−4397. (y) Zhang, L.-S.; Chen, G.; Wang, X.; Guo, Q.-Y.; Zhang, X.-S.; Pan, F.; Chen, K.; Shi, Z.-J. *Angew. Chem., Int. Ed.* **2014**, *53*, 3899−3903. (z) Seki, A.; Takahashi, Y.; Miyake, T. *Tetrahedron Lett.* **2014**, *55*, 2838−2841. (aa) Cheng, T.; Yin, W.; Zhang, Y.; Huang, Y. *Org. Biomol. Chem.* **2014**, *12*, 1405−1411. (ab) Gutekunst, W. R.; Baran, P. S. *J. Am. Chem. Soc.* **2011**, *133*, 19076−19079. (ac) Giri, R.; Maugel, N.; Foxman, B. M.; Yu, J.-Q. *Organometallics* **2008**, 1667−1670. (ad) Rit, R. K.; Yadav, M. R.; Sahoo, A. K. *Org. Lett.* **2012**, *14*, 3724−3727. (ae) Zhang, Q.; Chen, K.; Rao, W.; Zhang, Y.; Chen, F.-J.; Shi, B.-F. *Angew. Chem., Int. Ed.* **2013**, *52*, 13588−13592. (af) Zhang, Q.; Yin, X.-S.; Zhao, S.; Fang, S.-L.; Shi, B.-F. *Chem. Commun.* **2014**, *50*, 8353−8355. (ag) Rodríguez, N.; Romero-Revilla, J. A.; Fernández-Ibáñez, M. Á.; Carretero, J. C. *Chem. Sci.* **2013**, *4*, 175−179.. (ah) Cui, W.; Chen, S. W.; Wu, J.-Q.; Zhao, X.; Hu, W. H.; Wang, H. G. *Org. Lett.* **2014**, *16*, 4288−4291. (ai) Chen, K.; Zhang, S.-Q.; Xu, J.-W.; Hu, F.; Shi, B.-F. *Chem. Commun.* **2014**, *50*, 13924−13927. (aj) Zong, Y.; Rao, Y. *Org. Lett.* **2014**, *16*, 5278−5281. (ak) Affron, D. P.; Davis, O. A.; Bull, J. A. *Org. Lett.* **2014**, *16*, 4956−4959. (al) Fan, M.; Ma, D. *Angew. Chem., Int. Ed.* **2013**, *52*, 12152−12155. (am) Feng, R.; Wang, B.; Liu, Y.; Liu, Z.; Zhang, Y. *Eur. J. Org. Chem.* **2015**, 142−151. (an) He, G.; Zhang, S.-Y.; Nack, W. A.; Pearson, R.; Rabb-Lynch, J.; Chen, G. *Org. Lett.* **2014**, *16*, 6488−6491.

(14) C(sp^3)−H activation, Ru: (a) Hasegawa, N.; Charra, V.; Inoue, S.; Fukumoto, Y.; Chatani, N. *J. Am. Chem. Soc.* **2011**, *133*, 8070−8073. (b) Hasegawa, N.; Shibata, K.; Charra, V.; Inoue, S.; Fukumoto, Y.; Chatani, N. *Tetrahedron* **2013**, *69*, 4466−4472.

(15) C(sp^3)−H activation, Ni: (a) Aihara, Y.; Chatani, N. *J. Am. Chem. Soc.* **2014**, *136*, 898−901. (b) Wu, X.; Zhao, Y.; Ge, H. *J. Am. Chem. Soc.* **2014**, *136*, 1789−1792. (c) Li, M.; Dong, J.; Huang, X.; Li, K.; Wu, Q.; Song, F.; You, J. *Chem. Commun.* **2014**, *50*, 3944−3946. (d) Iyanaga, M.; Aihara, Y.; Chatani, N. *J. Org. Chem.* **2014**, *79*, 11933−11939. (e) Wu, X.; Zhao, Y.; Ge, H. *Chem.—Eur. J.* **2014**, *20*, 9530−9533. (f) Lin, C.; Yu, W.; Yao, J.; Wang, B.; Liu, Z.; Zhang, Y. *Org. Lett.* **2015**, *17*, 1340−1343.

DOI: 10.1021/acs.joc.5b00580
J. Org. Chem. 2015, 80, 4672−4682

(16) C(sp^3)−H activation, Fe: Shang, R.; Ilies, L.; Matsumoto, A.; Nakamura, E. *J. Am. Chem. Soc.* **2013**, *135*, 6030−6032.
(17) C(sp^3)−H activation, Cu: (a) Wu, X.; Zhao, Y.; Zhang, G.; Ge, H. *Angew. Chem., Int. Ed.* **2014**, *53*, 3706−3710. (b) Wu, X.; Zhao, Y.; Zhang, G.; Ge, H. *Chem.—Asian J.* **2014**, *9*, 2736−2739.
(18) N,O-bidentate auxiliary enabled C−H activation: (a) Wang, C.; Chen, C.; Zhang, J.; Han, J.; Wang, Q.; Guo, K.; Liu, P.; Guan, M.; Yao, Y.; Zhao, Y. *Angew. Chem., Int. Ed.* **2014**, *53*, 9884−9888. (b) Chen, L.-J.; Ren, B.; Li, L.-Y.; Yang, X.-Y.; Gong, J.-F.; Niu, J.-L.; Song, M.-P. *Org. Lett.* **2014**, *16*, 1104−1107. (c) Wang, Q.; Han, J.; Wang, C.; Zhang, J.; Huang, Z.; Shi, D.; Zhao, Y. *Chem. Sci.* **2014**, *5*, 4962−4967. (d) Zhang, L.-B.; Hao, X.-Q.; Zhang, S.-K.; Liu, Z.-J.; Zheng, X.-X.; Gong, J.-F.; Niu, J.-L.; Song, M.-P. *Angew. Chem., Int. Ed.* **2015**, *54*, 272−275. (e) Wang, M.; Yang, Y.; Fan, Z.; Chen, Z.; Zhu, W.; Zhang, A. *Chem. Commun.* **2015**, *51*, 3219−3222. (f) Zhou, X.; Wang, Q.; Zhao, W.; Xu, S.; Zhang, W.; Chen, J. *Tetrahedron Lett.* **2015**, *56*, 851−855.
(19) Tang, H.; Zhou, B. W.; Huang, X. R.; Wang, C. Y.; Yao, J. N.; Chen, H. *ACS Catal.* **2014**, *4*, 649−656.
(20) Frisch, M. J.; Trucks, G. W.; Schlegel, H. B.; Scuseria, G. E.; Robb, M. A.; Cheeseman, J. R.; Scalmani, G.; Barone, V.; Mennucci, B.; Petersson, G. A.; Nakatsuji, H.; Caricato, M.; Li, X.; Hratchian, H. P.; Izmaylov, A. F.; Bloino, J.; Zheng, G.; Sonnenberg, J. L.; Hada, M.; Ehara, M.; Toyota, K.; Fukuda, R.; Hasegawa, J.; Ishida, M.; Nakajima, T.; Honda, Y.; Kitao, O.; Nakai, H.; Vreven, T.; Montgomery, J. A., Jr.; Peralta, J. E.; Ogliaro, F.; Bearpark, M.; Heyd, J. J.; Brothers, E.; Kudin, K. N.; Staroverov, V. N.; Kobayashi, R.; Normand, J.; Raghavachari, K.; Rendell, A.; Burant, J. C.; Iyengar, S. S.; Tomasi, J.; Cossi, M.; Rega, N.; Millam, J. M.; Klene, M.; Knox, J. E.; Cross, J. B.; Bakken, V.; Adamo, C.; Jaramillo, J.; Gomperts, R.; Stratmann, R. E.; Yazyev, O.; Austin, A. J.; Cammi, R.; Pomelli, C.; Ochterski, J. W.; Martin, R. L.; Morokuma, K.; Zakrzewski, V. G.; Voth, G. A.; Salvador, P.; Dannenberg, J. J.; Dapprich, S.; Daniels, A. D.; Farkas, O.; Foresman, J. B.; Ortiz, J. V.; Cioslowski, J.; Fox, D. J. *Gaussian 09*, revision C.01; Gaussian, Inc.: Wallingford, CT, 2010.
(21) (a) Becke, A. D. *Phys. Rev. A* **1988**, *38*, 3098−3100. (b) Lee, C.; Yang, W.; Parr, R. G. *Phys. Rev. B* **1988**, *37*, 785−789. (c) Becke, A. D. *J. Chem. Phys.* **1993**, *98*, 5648−5652. (d) Becke, A. D. *J. Chem. Phys.* **1993**, *98*, 1372−1377. (e) Stephens, P. J.; Devlin, F. J.; Frisch, M. J.; Chabalowski, C. F. *J. Phys. Chem.* **1994**, *98*, 11623−11627.
(22) Weigend, F.; Ahlrichs, R. *Phys. Chem. Chem. Phys.* **2005**, *7*, 3297−3305.
(23) Marenich, A. V.; Cramer, C. J.; Truhlar, D. G. *J. Phys. Chem. B* **2009**, *113*, 6378−6396.
(24) Grimme, S.; Antony, J.; Ehrlich, S.; Krieg, H. *J. Chem. Phys.* **2010**, *132*, 154104.
(25) Fersht, A. *Structure and Mechanism in Protein Science: A Guide to Enzyme Catalysis and Protein Folding*; Freeman: New York, 1999.
(26) (a) Lai, W. Z.; Yao, J. N.; Sason, S.; Chen, H. *J. Chem. Theory Comput.* **2012**, *8*, 2991−2996. (b) Kang, R. H.; Lai, W. Z.; Yao, J. N.; Sason, S.; Chen, H. *J. Chem. Theory Comput.* **2012**, *8*, 3119−3127. (c) Kang, R. H.; Yao, J. N.; Chen, H. *J. Chem. Theory Comput.* **2013**, *9*, 1872−1879. (d) Sun, Y. Y.; Chen, H. *J. Chem. Theory Comput.* **2013**, *9*, 4735−4743. (e) Sun, Y. H.; Chen, H. *J. Chem. Theory Comput.* **2014**, *10*, 579−588. (f) Sun, Y. Y.; Hu, L. R.; Chen, H. *J. Chem. Theory Comput.* **2015**, DOI: 10.1021/ct5009119.
(27) It should be noted that unlike the 2-pyridinylmethylamine DG explored before in ref 19, for all the bidentate DGs in **1a**−**5a** for reactions 1−5, there is no straightforward way to reduce the chelating ring size without substantial change of the chemical structure of DGs. Thus in this work we did not explore the effect of four-membered ring.

DOI: 10.1021/acs.joc.5b00580
J. Org. Chem. 2015, 80, 4672−4682